Proc. Natl. Acad. Sci. USA
Vol. 83, pp. 8977–8981, December 1986
Biophysics

Fluorescence polarization decay of tyrosine in lima bean trypsin inhibitor

(protein motions/anisotropy decay/picosecond spectroscopy/Bowman–Birk protease inhibitor)

THOMAS M. NORDLUND*†‡, XIAO-YUAN LIU†, AND JOSEPH H. SOMMER*†§

*Department of Biophysics, Medical Center, University of Rochester, Rochester, NY 14642; †Department of Physics and Astronomy, University of Rochester, Rochester, NY 14627; and ‡Laboratory for Laser Energetics, University of Rochester, Rochester, NY 14623

Communicated by Hans Frauenfelder, August 25, 1986

ABSTRACT **The fluorescence of lima bean trypsin inhibitor is due to a single tyrosine residue at position 69. The lifetime of this tyrosine fluorescence is 620 ± 50 ps (mean ± SD) and is little affected by addition of 0.88 M citrate, an efficient quencher of tyrosine fluorescence. The steady-state emission intensity is also only weakly reduced by the quencher. The tyrosine is thus not accessible to the citrate and is probably located in the interior of the protein. The high pK of the tyrosine supports this conclusion. The fluorescence anisotropy decay of the inhibitor's tyrosine can be fitted to a double exponential form, with time constants of about 40 ps and ≥ 3 ns. The anisotropy at time zero is 0.19 ± 0.015 (mean ± SD), the same as for *N*-acetyl-L-tyrosinamide in viscous glycerol solution. The nanosecond component of the decay is consistent with rotation of the entire protein molecule. The 40-ps component demonstrates that the tyrosine has considerable freedom to move independently of the protein as a whole. This rotational correlation time is approximately what is observed for free tyrosine in aqueous solution. Since the polypeptide chain near tyrosine-69 is anchored by several disulfide bonds, the data argue that this interior portion of the protein consists of a rigid, immobile backbone embedded in fluid, mobile amino acid side chains.**

Proteins undergo structural fluctuations and motions that may range in time scale from picoseconds or less to hours or more. Evidence for ultrafast motions has been found in fluorescence, NMR, IR, Raman, and flash photolysis spectroscopic data and in computer molecular dynamics simulations of the motions of individual atoms or amino acid side chains (e.g., see refs. 1–9). The functional properties of some, and perhaps all, proteins depend upon these motions. One simple example of this fact is that neither hemoglobin nor myoglobin could bind oxygen unless the protein structure fluctuated to allow the oxygen to pass through to the heme site (10, 11).

Early theoretical studies of rapid protein motions concentrated on bovine pancreatic trypsin inhibitor (BPTI). Subsequent work, both theoretical and experimental, has been done on a variety of other proteins. BPTI has been an attractive protein because of its well-characterized crystal structure and its relatively small size (6, 7, 12). BPTI is a compact protein of 58 amino acids, with three disulfide bonds, four tyrosine residues, and no tryptophan. Fluorescence from the tyrosine residues has been used to experimentally study protein fluctuations using steady-state polarization methods (3). A connection between these experiments and the computer simulations has also been made (13). However, the only conclusion that could be made was that there existed a "short-time" depolarization, which could be consistent with the 0.5- to 1-ps rotational correlation time found from the simulation (3). Energy transfer could also have accounted for the measured depolarization and the rate of polarization decay was not determined. The energy transfer problem is caused by the fact that BPTI has four tyrosines. We have chosen to study a relative of BPTI, lima bean trypsin inhibitor (LBTI), which has a single tyrosine and no tryptophan. There is little apparent sequence homology between these two inhibitors, though they are similar in their lack of tryptophan, their low molecular mass, and their relatively high disulfide content. LBTI has 83 amino acids, molecular mass about 9 kDa, and seven disulfide bonds. The amino acid sequence and disulfide bond structure of LBTI are known, but the crystal structure has not yet been solved. X-ray diffraction patterns from crystals of homologous inhibitors have been published (14–16).

The disulfide interconnections in LBTI keep the polypeptide backbone near Tyr-69 rigid, as the schematic of Fig. 1 illustrates. It is also clear that the backbone structure of the protein is relatively well-defined by the disulfides except for the 17 amino-terminal residues, the 11 carboxyl-terminal residues, and the interconnecting links between the trypsin active site (loop 24–32) and the chymotrypsin active site (loop 51–59). The observation that trypsin and chymotrypsin bind to LBTI noncompetitively (15) implies that the two sites are not close together. For present purposes, however, it is sufficient to note the rigid backbone mount of the Tyr-69 side chain.

LBTI, like a number of other so-called Bowman–Birk protease inhibitors, is isolated chromatographically as a series of four to six polypeptides, each of which apparently has a slightly different amino acid sequence (17, 18). Several of the LBTI proteins have been sequenced by Stevens *et al.* as well as tested for enzymatic activity (18). Inhibitory activities toward trypsin are very similar for the inhibitor fractions tested, though activities toward chymotrypsin are measurably different, presumably because of the different LBTI sites involved. The binding sites for trypsin and chymotrypsin are Lys-26–Ser-27 and Leu-53–Ser-54, respectively. Sequences of the fractions differ in the first 13 amino-terminal residues. Some of the fractions apparently lack a number of amino acids. From position 13 on, however, almost complete homology between the fractions is observed. The region we are particularly interested in is near Tyr-69. This region is identical for the inhibitor fractions sequenced. Residue 70 is a glutamate, which is negatively charged. This will be of importance for later considerations of fluorescence quenching by a negatively charged ion.

This paper describes the fluorescence anisotropy decay of Tyr-69 in LBTI using a signal-averaging laser-streak camera

The publication costs of this article were defrayed in part by page charge payment. This article must therefore be hereby marked "*advertisement*" in accordance with 18 U.S.C. §1734 solely to indicate this fact.

Abbreviations: LBTI, lima bean trypsin inhibitor; BPTI, bovine pancreatic trypsin inhibitor; $AcTyrNH_2$, *N*-acetyl-L-tyrosinamide; Nd:YAG, neodymium^{3+}:yttrium/aluminum/garnet.

§Present address: P.O. Box 6123, Yale Station, New Haven, CT 06520.

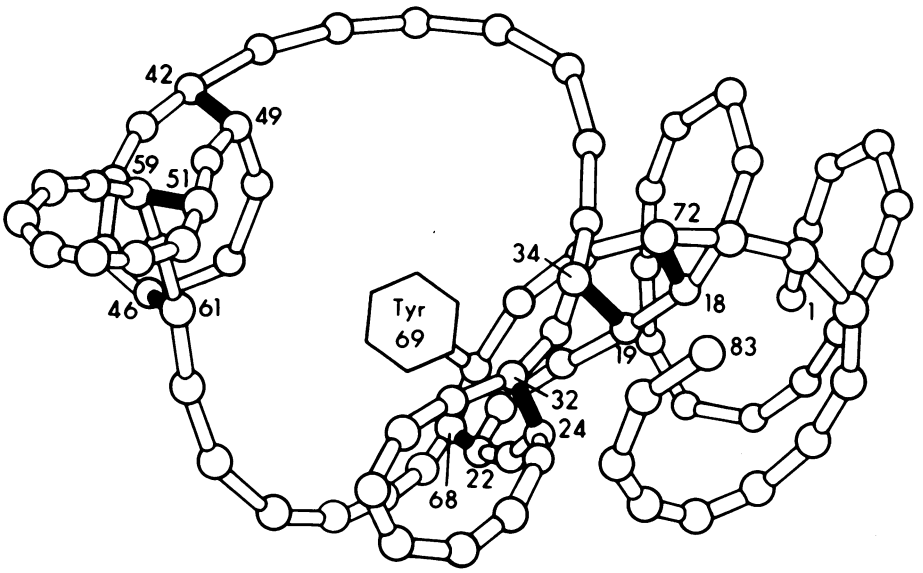

FIG. 1. Schematic of LBTI showing Tyr-69 and the seven disulfide bonds in their proper places. The spheres indicate the α-carbons of each amino acid.

system capable of resolving protein fluorescence anisotropy decays as short as tens of picoseconds. By comparison with the anisotropy decay of *N*-acetyl-L-tyrosinamide (AcTyr-NH_2) in a viscous solution, conclusions are made as to the likelihood of tyrosine motions unique to LBTI on a time scale shorter than 10 ps.

FLUORESCENCE ANISOTROPY

In a time-resolved fluorescence anisotropy experiment a polarized excitation pulse excites fluorophores, which subsequently emit. The time-dependent emission anisotropy is defined as

$$r(t) = [I \parallel (t) - I_{\perp}(t)]/[I \parallel (t) + 2I_{\perp}(t)], \quad [1]$$

where $I \parallel$ ($I_{\perp}$) is the fluorescence polarized parallel (perpendicular) to the polarization direction of the excitation beam. After excitation the fluorophores may be free to rotate, in which case the anisotropy will decrease with time. If the decay of the total fluorescence is a simple exponential process and no energy transfer takes place, then the shape of the anisotropy decay curve will be governed by the rotational behavior of the emitter. If the sample is a protein with a single fluorophore, then at least one rotational correlation time corresponding to rotation of the whole protein should be observed. This correlation time will generally be longer than 1 ns. If an anisotropy component decays in less than about 1 ns, then under our assumptions the emitter must be moving independently of the protein as a whole.

For a fluorophore that has rotational freedom within the protein the time-resolved anisotropy can be approximated as a double-exponential decay,

$$r(t) = r_0 e^{-t/\phi} [ae^{-t/\phi_i} + (1 - a)], \quad [2]$$

where ϕ is the rotational correlation time for the protein as a whole, ϕ_i is that for the internal motion, and a is the fraction of the total anisotropy that decays as a result of the internal motion. In this simple model the decays of $r(t)$ due to overall protein rotation and to internal motion are each assumed to be exponential in time and the two motions are assumed to be independent.

The initial value of the anisotropy in Eq. 2 is r_0 and the value is 2/5 if the absorption and emission dipoles are parallel. If the two dipoles are at an angle then the initial anisotropy is less. This reduction of r_0 due to the geometrical arrangement of the two transition dipoles can be mimicked by a fluorophore rotation that is much too fast for the measuring apparatus to revolve. It is therefore desirable to have a way to distinguish between the two effects. We attempt this by using a reference molecule ($AcTyrNH_2$) of controllable rotation rate.

MATERIALS AND METHODS

The fluorescence of LBTI was excited by using the fourth harmonic of a Q-switched, mode-locked, single-pulse selected neodymium^{3+}:yttrium/aluminum/garnet (Nd:YAG) laser, which produced a 0.5- to 1.0-μJ, 30-ps pulse at 266 nm. A signal-averaging streak camera-optical multichannel analyzer system was used to detect the emission and determine the anisotropy as a function of time. The entire system has been described in detail elsewhere (19–23). The excitation beam was focused to 0.3 mm minimum diameter with a 20-cm focal length fused silica lens. The emission was viewed at an angle 90° to the excitation beam direction. The solid angle collected was about 3 millisteradians. Schott WG305 and UG11 glass filters were used to cut out scattered excitation and stray light. Each filter was 2 mm thick. The pass band of the filter combination was 300- to 380-nm full-width-half-maximum. The energy of each laser pulse was monitored by a photodiode-op amp combination (model HUV1000B, E.G. & G., Salem, MA) connected to a peak-reading voltmeter (Nanofast model 562-40A, Chicago, IL). Most of the data shown in this paper were taken by separately measuring the total emission excited by vertically polarized and by horizontally polarized light, correcting for laser energy fluctuations. Some data were recorded using a dual-channel method similar to that described in ref. 22.

The first lot of LBTI was purchased from Cooper Biomedical/Worthington (Freehold, NJ) and used without further purification for the kinetic data reported here. This lot (51N520) was relatively pure, as measured by its activity, 2.8 mg of trypsin inhibited per mg of LBTI (Worthington's determination), and by its fluorescence spectrum (our measurement). Two subsequent lots, N1P563 and 55C7504, had lower activity, 2.3 mg per mg, and showed a large emission shoulder in the 350-nm region in addition to the main tyrosine peak at 302 nm. We have determined from absorption and

fluorescence excitation and emission spectra of Sephadex G-75-purified samples (24) that this 350-nm band is probably due to tyrosinate (25–28) emission. We find that inhibitor molecules that apparently have one or more disulfide bonds ruptured emit significantly at wavelengths characterizing tyrosinate (X.-Y.L., T.M.N., and K. Cottrell, unpublished). Szabo *et al.* observed tyrosinate emission from cobra cytotoxins, which, like LBTI, are low molecular mass proteins containing disulfide cross-links and tyrosine but no tryptophan (28). In their study, however, tyrosinate emission was abolished when the disulfides were broken and carboxymethylated. The time-resolved fluorescence and anisotropy signals we observed were thus probably not from a single species, since some 350-nm emission occurred in addition to the primary 302-nm band. The fluorescence filters we used could not completely isolate the 302-nm emission. The decay of the total fluorescence in Fig. 2 appears exponential, but a small, short-lived tyrosinate (26) component cannot be ruled out. Any tyrosinate that is emitting would generally be expected to exhibit a rotational correlation time slower than that of tyrosine, since tyrosinate is formed only when the phenol group has an additional interaction with a proton-accepting group.

The solutions were buffered with 0.02 M bis-Tris·HCl (pH 6.5) with 0.15 M NaCl. The sample was placed in a 3 × 3 mm Suprasil fluorescence cuvet for the kinetic measurements, with a solution optical density of 0.2–0.3 at the 273-nm absorption peak. The excitation beam axis was located about 1 mm from the detector's side of the cuvet. $AcTyrNH_2$ was purchased from Sigma and the dipeptide Tyr-Glu and tripeptide Leu-Tyr-Leu were from Serva (Westbury, NY). The temperature was controlled at 23°C in the kinetic experiments. Steady-state measurements were done at room temperature (23 ± 1°C).

The anisotropy was calculated (22) as

$$r(t) = (I^v - I^h)/(I^v + 0.5I^h), \quad [3]$$

where I^v is the total signal observed with a vertically polarized excitation pulse and I^h is the total signal observed with a horizontally polarized excitation pulse. The decay of the total fluorescence is just the denominator of Eq. 3. This expression is equivalent to the definition in Eq. 1.

RESULTS

The decay of the total fluorescence of LBTI is shown in Fig. 2. The decay curve is approximately single exponential over the time scale of our observations, with a lifetime of 620 ± 50 ps (mean ± SD). Citrate is an efficient quencher of tyrosine fluorescence when the citrate has access to the tyrosine (3). The quenching mechanism is believed to be static in nature. Addition of citrate to the LBTI solution should therefore reduce the fluorescence unless the tyrosine is inaccessible. Addition of up to 0.8 M sodium citrate at constant pH to our sample solutions did not affect the decay rate. The total amplitude of the time-resolved fluorescence signal decreased by about 35% with added 0.8 M citrate.

Steady-state quenching experiments were carried out on LBTI and several model compounds to assess the influence of the tyrosine surrounding upon the ability of citrate to quench the fluorescence. The citrate concentrations needed to quench 50% of the fluorescence of LBTI, the Leu-Tyr-Leu tripeptide, the Tyr-Glu dipeptide, and $AcTyrNH_2$ were 0.85, 0.34, 0.21, and 0.14 M, respectively. These data and those in the following paragraph will be published in complete form elsewhere.

The pH at which the Tyr-69 hydroxyl group ionizes is also an indicator of the accessibility of the tyrosine to protons from the solvent. We observe the pK of tyrosine in LBTI to be at least 11.1, 1.1 pH units higher than those of Leu-Tyr-Leu, Tyr-Glu, and $AcTyrNH_2$, using the red shift of the absorption spectrum as a measure of the tyrosine ionization.

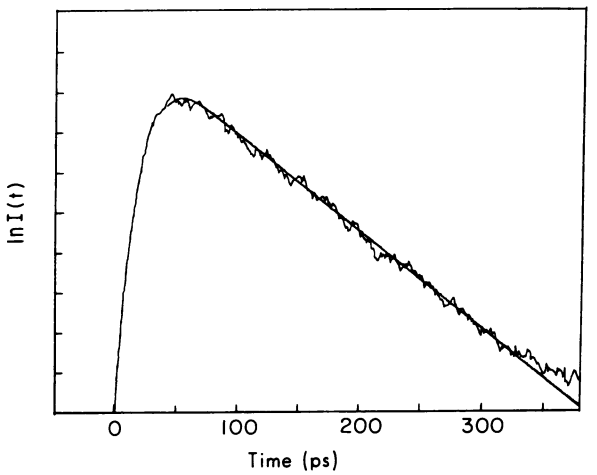

FIG. 2. Fluorescence decay of LBTI. The curves are $I^v + 0.5I^h$, the total fluorescence emission, plotted on a semilogarithmic scale. Each vertical division is 0.08. The jagged curve is the signal. Three hundred laser shots were summed for each excitation polarization direction. The smooth curve is a single-exponential computer fit, with a lifetime of 620 ps.

The emission anisotropy decay of LBTI, shown in Fig. 3, has two components. The slowly and quickly decaying components have amplitudes 0.072 ± 0.013 and 0.118 ± 0.015 (mean ± SD), respectively, and rotational correlation times ≥3 ns and 40 (+30, −10) ps, respectively. The smooth curve in Fig. 3 is a fit of Eq. 2 to the anisotropy data, found by the computer when it was given a fixed r_0 and fluorescence decay time of 0.19 and 650 ps, respectively, and instructed to find a best least-squares fit by varying ϕ, ϕ_i, and a. The computer convolved the laser excitation pulse with the double-exponential form for the decay of the anisotropy to generate I^v and I^h and fit the experimental curve for $r(t)$.

$AcTyrNH_2$ is a good model compound for studying the fluorescence anisotropy behavior of tyrosine residues in proteins. The α-carbon is bonded as is tyrosine in a polypeptide, leaving no charged groups, and the fluorescence behavior has been studied (29). If $AcTyrNH_2$ is placed in a viscous solvent it might be expected that any rotations of the

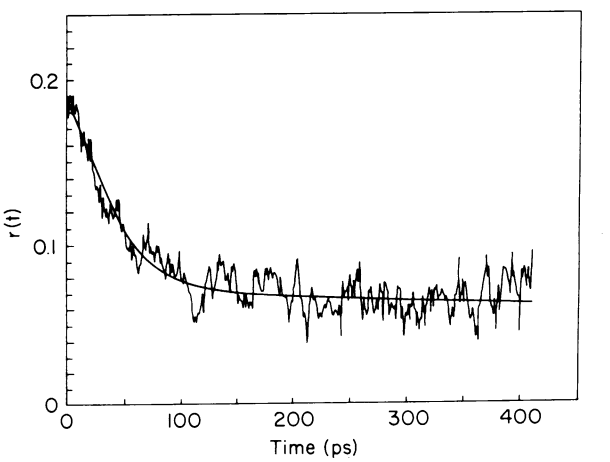

FIG. 3. Anisotropy decay of LBTI. Time zero is the time corresponding to the center of the excitation pulse. Data, jagged curve; fit, smooth curve. Three hundred shots were summed for each polarization component. The fit was done by a computer least-squares routine using Eq. 2.

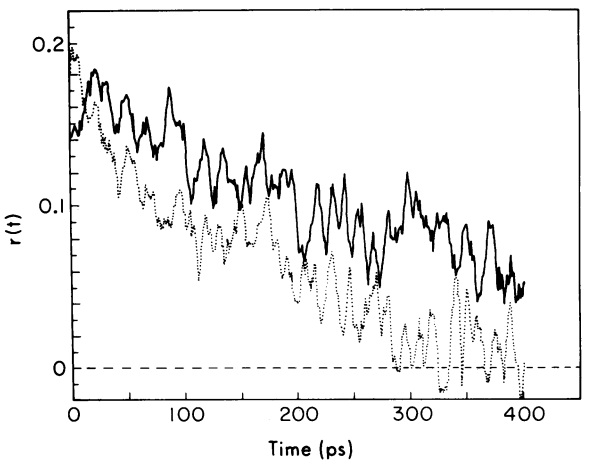

FIG. 4. Anisotropy decay of $AcTyrNH_2$ in 40% (dotted curve) and 50% (solid curve, % by volume) glycerol/water solution at 23°C. One hundred shots were summed for each polarization component. The limiting value of $r(t)$ at time zero is 0.18 ± 0.02.

phenol ring could be slowed to any desired degree, depending upon the viscosity. In this way the maximum value of the anisotropy could be determined, as any picosecond rotations that may occur at room temperature in aqueous solution could be slowed into the 100-ps or longer time range, which is easily accessible to our apparatus. The fluorescence anisotropy of $AcTyrNH_2$ in 40% and 50% (vol/vol) glycerol/water solution is plotted in Fig. 4, which shows an anisotropy decay time of about 350 ps for the less viscous solution and a slower decay at higher viscosity. Both decay curves have a maximum value, $r(0)$, of 0.18 ± 0.02. This is the same as that observed for LBTI, within experimental error.

DISCUSSION

Tyr-69 in LBTI is most likely buried within the protein where it is protected from the solvent. This is suggested by two independent lines of evidence: the observed weak dependence of the fluorescence on citrate concentration and the high pK of Tyr-69. The possibility that the tyrosine is not buried but merely shielded by the negatively charged Glu-70 is unlikely because of the much smaller citrate concentration needed to produce comparable quenching in Tyr-Glu. Four times as much citrate is needed for 50% quenching of LBTI as for the Tyr-Glu dipeptide. Further, the fact that the Tyr-Glu dipeptide is more readily quenched than the Leu-Tyr-Leu tripeptide implies that steric effects of the neighboring amino acids are more important than charge effects in hindering the approach of the citrate ion to the tyrosine. The high pK of Tyr-69 shows that the group is not easily accessible to solvent protons. The lability of disulfide bonds at high pH (30) indeed suggests that Tyr-69 cannot be ionized until the protein is denatured. Thus, the motions that we discuss appear to be those of a group that is effectively surrounded by protein structure.

The motions of Tyr-69 give rise to two anisotropy decay processes. The slow $\geq$3-ns process is consistent with what the Debye–Stokes–Einstein theory (31) predicts for the rotational correlation time of a 9-kDa (spherical) protein molecule, about 3.9 ns. The second anisotropy decay process has a fast decay time, about 40 ps. This is comparable to the rotational correlation times observed for tryptophan and tyrosine in aqueous solution at room temperature (4, 22, 29). If we assume that the tyrosine emission dipole moves in a square potential well, where the potential is infinite outside of the angular range $\pm\beta$ and flat within that range (1, 13, 32), then we find $\beta \approx 45°$. Though this model is undoubtedly not accurate, it illustrates the fact that this "buried" tyrosine is relatively free to rotate.

Given the coincidence between the rotational correlation times of tyrosine in LBTI and in aqueous solution, it is tempting to suggest that the LBTI tyrosine ring is in a local interior environment with the viscosity of water. The motion may be constrained only by the protein backbone, at the α-carbon of Tyr-69, and by the potential well walls. If this picture were generally true, it would considerably simplify the problems of protein dynamics to the motions of protein backbones and atoms rigidly coupled to them. However, this picture is apparently too simple to be generally applicable. The size of the amino acid side chain and/or its particular environment in a protein interior seem to affect how free the side chain is to rotate (1, 3, 6–8). In human serum albumin, for example, the tryptophan displays no motion consistent with the fluid-like but backbone-constrained motion postulated for the LBTI tyrosine except at elevated temperature (1, 22). Ohgushi and Wada have concluded that side chains are generally in a fluid state at intermediate states of protein denaturation (33). Munro *et al.* observed that the buried tryptophan of azurin displays motional freedom independent of the protein as a whole at room temperature, but the rotational correlation time was 510 ps, significantly longer than that observed for tryptophan in water (1). The dependence of motional freedom on molecular size has been discussed in this and in other contexts by a number of authors (e.g., refs. 7, 34, 35).

Are there any subpicosecond motions of Tyr-69 in LBTI that we cannot resolve? The equality of the apparent r_0 values for LBTI and $AcTyrNH_2$ in glycerol or aqueous solutions suggests there are not. However, it is possible that $AcTyrNH_2$ as well as Tyr-69 undergo motions not predicted by Debye–Stokes–Einstein theory. Molecular motions of groups as large as methylene apparently can occur even at the extreme limit of viscosity—solids at low temperatures (36, 37)—so the possibility of subpicosecond rotations of tyrosine in glycerol or in LBTI cannot be ruled out altogether. The only safe conclusion, in the absence of reliable frozen matrix data, is that any subpicosecond motions of tyrosine are of similar magnitude in the protein and the solvent.

In conclusion, we have observed a biphasic decay of the fluorescence anisotropy of the single tyrosine in LBTI. The slow phase can be ascribed to overall protein rotation in the solvent. The fast phase is consistent with constrained rotation of the tyrosine in an environment with an apparent viscosity similar to that of water.

We thank K. Cottrell for experimental assistance. This work was supported in part by National Science Foundation Grants PCM 83-02601, 83-03004, and 80-18488 and by the sponsors of the Laser Fusion Feasibility Project at the Laboratory for Laser Energetics of the University of Rochester.

1. Munro, I., Pecht, I. & Stryer, L. (1979) *Proc. Natl. Acad. Sci. USA* **76**, 56–60.
2. Petrich, J. W. & Fleming, G. R. (1984) *Photochem. Photobiol.* **40**, 775–780.
3. Kasprzak, A. & Weber, G. (1982) *Biochemistry* **21**, 5924–5927.
4. Gratton, E. & Barbieri, B. (1986) *Spectroscopy* **1(6)**, 28–38.
5. Gurd, F. R. N. & Rothgeb, T. M. (1979) *Adv. Protein Chem.* **33**, 73–165.
6. Levitt, M. (1983) *J. Mol. Biol.* **168**, 595–657.
7. Karplus, M. & McCammon, J. A. (1981) *CRC Crit. Rev. Biochem.* **9**, 293–349.
8. Karplus, M. (1984) *Adv. Biophys.* **18**, 165–190.
9. Sarma, R. H., ed. (1981) *Biomolecular Stereodynamics* (Adenine Press, New York).
10. Perutz, M. F. & Matthews, F. S. (1966) *J. Mol. Biol.* **21**, 199–202.
11. Frauenfelder, H., Petsko, G. A. & Tsernoglou, D. (1979)

Nature (London) **280,** 558–563.
12. Huber, R., Kukla, D., Rühlmann, A. & Steigemann, W. (1971) in *Proceedings of the International Research Conference on Proteinase Inhibitors*, eds. Fritz, H. & Tschesche, H. (de Gruyter, Berlin), pp. 56–65.
13. Levy, R. M. & Szabo, A. (1982) *J. Am. Chem. Soc.* **104,** 2073–2075.
14. Wei, C. H. (1983) *J. Biol. Chem.* **258,** 9357–9359.
15. Birk, Y. (1985) *Int. J. Pept. Protein Res.* **25,** 113–131.
16. Gaier, J. R., Tulinsky, A. & Liener, I. E. (1981) *J. Biol. Chem.* **256,** 11417–11419.
17. Ketcham, L. K., Barker, W. C. & Dayhoff, M. O. (1978) in *Atlas of Protein Sequence and Structure*, ed. Dayhoff, M. O. (Natl. Biomed. Res. Found., Washington, DC), p. 136.
18. Stevens, F. C., Wuerz, S. & Krahn, J. (1974) in *Proteinase Inhibitors*, eds. Fritz, H., Tschesche, H., Greene, L. J. & Truscheit, E. (Springer, New York), pp. 344–354.
19. Mourou, G. & Knox, W. (1980) *Appl. Phys. Lett.* **36,** 623–626.
20. Knox, W. & Mourou, G. (1981) *Opt. Commun.* **37,** 203–206.
21. Stavola, M., Mourou, G. & Knox, W. (1980) *Opt. Commun.* **34,** 404–408.
22. Nordlund, T. M. & Podolski, D. A. (1983) *Photochem. Photobiol.* **38,** 665–669.
23. Sommer, J. H., Nordlund, T. M., McGuire, M. & McLendon, G. (1986) *J. Phys. Chem.* **90,** 5173–5178.
24. Jones, G., Moore, S. & Stein, W. H. (1963) *Biochemistry* **2,** 66–71.
25. Shimizu, O. & Imakubo, K. (1977) *Photochem. Photobiol.* **26,** 541–543.
26. Lakowicz, J. R. (1983) *Principles of Fluorescence Spectroscopy* (Plenum, New York), pp. 359–363.
27. Wetlaufer, D. B. (1962) *Adv. Protein Chem.* **17,** 303–390.
28. Szabo, A. G., Lynn, K. R., Krajcarski, D. T. & Rayner, D. M. (1978) *FEBS Lett.* **94,** 249–252.
29. Lakowicz, J. R. & Maliwal, B. P. (1983) *J. Biol. Chem.* **258,** 4794–4801.
30. Donovan, J. W. (1973) *Methods Enzymol.* **27,** 497–548.
31. Perrin, F. (1936) *J. Phys. Radium.* **7,** 1–11.
32. Lipari, G. & Szabo, A. (1980) *Biophys. J.* **30,** 489–506.
33. Ohgushi, M. & Wada, A. (1984) *Adv. Biophys.* **18,** 75–90.
34. Calhoun, D. B., Vanderkooi, J. M., Woodrow, G. V. & Englander, S. W. (1983) *Biochemistry* **22,** 1533–1539.
35. Sommer, J. H., Henry, E. R. & Hofrichter, J. (1985) *Biochemistry* **24,** 7380–7388.
36. Henry, E. R. & Szabo, A. (1985) *J. Chem. Phys.* **82,** 4753–4761.
37. Soulard, L., Fillaux, F., Braathen, G., Le Calve, N. & Pasquier, B. (1986) *Chem. Phys. Lett.* **125,** 41–46.